Development of an Improved Model for Piezo-Electric Driven Ink Jets

Sharon S. Berger
Xerox Corporation, Wilsonville, Oregon

Gerald Recktenwald
Portland State University, Portland, Oregon

Abstract

Numerical modeling and experimentation are used at Xerox Office Group to design, optimize, and verify the fluid dynamic behavior of phase-change ink jets, including the individual jets in a print head. A typical model of an ink jet is based upon lumped-parameter (no spatial variation) assumptions. While quite accurately predicting the main Helmholz resonant frequency (a key performance measure), a lumped-parameter model does not predict other parasitic frequencies that occur in a typical ink jet. As printer performance improves by increasing the jetting frequency, understanding and controlling these other resonant frequencies becomes critical. This paper documents the improvement of an existing lumped-parameter model by incorporating one-dimensional transmission line elements which substantially increases the ability of the model to predict the frequency response of an ink jet.

The first part of the paper describes the application of lumped-parameter elements and of transmission line theory to the modeling of ink jets. The existing lumped-parameter model and the improved model are then used to simulate a Xerox Phaser® 350 ink jet. The model predictions are compared with experimental data obtained with an impedance meter.

Introduction

Frequency-domain solutions can help to rapidly determine the overall frequency and damping characteristics of an ink jet design. Knowing where the resonance frequencies are is crucial to predicting jet performance. The frequency and damping of the Helmholz mode are key design parameters that define the maximum possible firing rate. As the firing rate of the jets increases, higher resonant frequencies can affect the quality of the printed image.

As a print head prints an image, an ink jet can print at maximum operating frequency (i.e. in a solid fill color) or at any one of the sub-harmonics of the maximum frequency (i.e. in text or a light fill color), often printing only a few drops at every frequency. For ideal print quality, the drop size and velocity should not vary with frequency. For firing frequencies below 20 percent of Helmholz frequency, the drop is usually independent of frequency. As the firing frequency increases, resonance nodes and antinodes from any ink jet resonant frequencies introduce variations in drop size and velocity. This is mainly because energy from the driving waveform can excite not only the Helmholz resonance mode, which is desired for efficiency, but other resonance modes as well.

Accurately predicting these higher frequency resonant modes will allow for both drive waveform and geometry changes in the design process to mitigate or eliminate these resonance modes and keep them from affecting print quality. Typically, these higher resonance modes are due to wave propagation effects. By increasing the model dimension to one-dimension for the appropriate ink jet features, wave propagation effects can be included.

Model Development

The lumped-parameter assumption is that the characteristic wavelength is larger than all dimensions in a pipe. This assumption is valid for pipes where the frequency (f) is much less that the transmission time, defined as the sound speed, a, divided by the length, ℓ (f<< a/ℓ). Physically what the lumped-parameter assumption means is that the fluid in the flow direction is uniform at any instant in time. In the lumped-parameter model, the flow is also assumed to be acoustic in nature: the fluctuations are small compared to ambient conditions, and the walls of the pipe are stiff relative to the fluid.

Three parameters can be derived to describe the behavior of fluid in a lumped element. These are the lumped inertia or inductance (L), lumped capacitance (C) and resistance (R). The inertia is related to the fluid mass, the capacitance is a measure of fluid energy storage and elasticity and the resistance is associated with any losses causing energy dissipation in the fluid, typically viscous losses.

The inductance and resistance are derived from the conservation of momentum and the capacitance from the conservation of mass.[2] The expressions for these fluid parameters are now presented without further details. The inductance is given by

$$L = \beta \, \frac{\ell}{S} \qquad (1)$$

where ℓ is pipe length, S is the cross-sectional area and β is a constant that corrects for momentum differences due the velocity profile.[1] The resistance in a pipe is given by

$$R = \frac{128\mu\ell}{\rho\pi D^4} \qquad (2)$$

where μ is the viscosity, ρ is the density and D is the pipe diameter. The capacitance is given by

$$C = \frac{S\ell}{a^2} \qquad (3)$$

where a is the sound speed.

In acoustic flows, the fluctuations in the field variables (pressure, density and velocity) normally are small with respect to ambient. These small fluctuations can be written as an ambient value plus a perturbation. Using these time-dependent fluctuating acoustic properties, a single expression for pipe input pressure as a function of mass flow rate can be written as

$$p = R\dot{m} + j\omega L\dot{m} + \frac{1}{j\omega C}\dot{m} \qquad (4)$$

j=sqrt(-1) and ω is the angular frequency. It is convenient to use an electrical analogue to write the Equation (4) as acoustic impedance, Z. Acoustic impedance is typically a frequency domain expression defined as the acoustic pressure divided by the volume velocity [3, p. 321][4, p. 320]. We use mass flow rate rather than volume velocity. The resulting equation is

$$Z = \frac{p}{\dot{m}} = R + j\left(\omega L - \frac{1}{\omega C}\right) \qquad (5)$$

where R, L, and C are the lumped-parameters defined in Equations (1) through (3).

When one dimension of a fluid element is not small compared with the wavelength, it is not accurate to treat that geometry as a lumped element. In pipes with a cross-sectional area much smaller than the wavelength of the sound wave, the fluid density and pressure vary only along the pipe axis and the motion is called a plane wave. This motion is analogous to electric current flowing along a wire and thus can be written in the same form as the transmission-line equations.

The wave equation for inviscid linear acoustic flows is derived in numerous texts[2-5] and is given by

$$\frac{\partial^2 p'}{\partial z^2} - \frac{1}{a^2}\frac{\partial^2 p'}{\partial t^2} = 0 \qquad (6)$$

We can write Equation (6) with electrical analogies as

$$\frac{\partial^2 p'}{\partial z^2} - L'C'\frac{\partial^2 p'}{\partial t^2} = 0 \qquad (7)$$

The capacitance and inductance in Equation (7) are distributed quantities (e.g. per unit length) [2, p. 290][3, p. 233][5, pp. 474-475]. We previously presented fluid analogies for lumped elements (Equations (1) and (3)). To convert these lumped-parameter values to distributed values, we divide by the length. The equations of inductance and compliance per unit length are

$$L' = \frac{L}{\ell} = \frac{\ell}{S\ell} = \frac{1}{S} \qquad (8)$$

$$C' = \frac{C}{\ell} = \frac{S\ell}{a^2\ell} = \frac{S}{a^2} \qquad (9)$$

The solution to the wave equation, Equation (7), is obtained assuming a harmonic wave oscillation.[3] By combining the equations for each end of the pipe, we obtain a single expression for pipe input impedance. This is often written in the following form

$$Z_o = z \frac{Z_\ell/z + j\,tan(\omega\sqrt{L'C'}\ell)}{1 + j\,Z_\ell/z\,tan(\omega\sqrt{L'C'}\ell)} \qquad (10)$$

With the appropriate substitutions for the end impedance, Z_ℓ, the acoustic impedance Z_0 can be determined for plane wave flow in a pipe.

Model Implementation

A typical ink jet geometry for a Xerox phase-change ink jet (see Figure 1) generally consists of an inlet, an outlet, a driving chamber, and an aperture. The inlet pulls ink from a manifold. The ink feeds from the inlet into the body (the fluid portion of the driving chamber). The outlet connects the body to the aperture. The ink drop is ejected from the aperture to the printing surface. The expansion and contraction of the piezo-electric transducer (PZT) attached to the wall of the body generates a pressure wave that produces the ink drops.
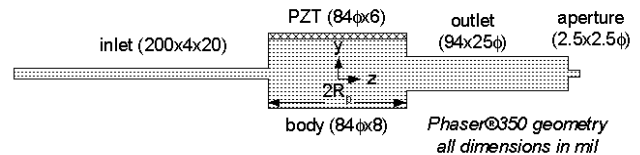

Figure 1. Simplified representation of a typical ink jet geometry

In the lumped-parameter model, each feature described in Figure 1 has lumped-parameter values associated with it. The inlet is described with resistance (R), capacitance (C) and inductance (L) values. The body is modeled using capacitance only. The outlet is modeled with R, C and L elements, similar to the inlet. The aperture is a much smaller

ink volume than the rest of the ink jet thus the capacitance is ignored and only R and L elements are used.

Other components of the ink jet are also modeled by casting their behavior into lumped parameters. Among these are the inlet boundary condition, mechanical coupling of the piezo-electric element to the body and the meniscus in the aperture. At the inlet, the boundary condition used is that of a flanged pipe opening into space [3, p. 202] [4, p. 349]. The mechanical model of the piezo-electric transducer attached to the diaphragm is substantially based a paper written by Roy et al.[6] The meniscus is modeled solely as a capacitor. The meniscus capacitance is found from a force balance on a hemisphere of fluid that has an air interface[1, p. 31].

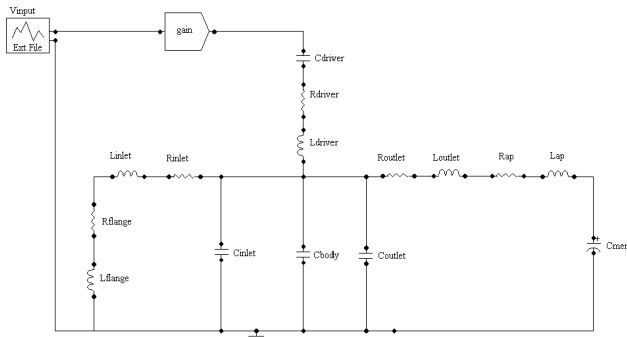The schematic of the lumped-parameter model of the ink jet is given in Figure 2.

Figure 2. Schematic of lumped-parameter ink jet model

The geometries of the inlet and outlet in Figure 1 suggest that to improve the ink jet model's accuracy, the delay time down the length of the inlet and outlet need to be accounted for. In other words, these portions of the jet geometry should be modeled with a transmission line rather than lumped-parameters. The RLC parameters for the inlet and the outlet are easily replaced with transmission line equations in the model.

The body is another portion of the ink jet model that could be improved. In developing the lumped-parameter model, an assumption was made that the flow direction is the depth of the body (the y-direction in Figure 1 which is 8 mil in the Phaser® 350). It is quite conceivable that a resonance mode would exist where a wave could travel from the inlet to the outlet across the width of the body ($2R_p$ in Figure 1). This dimension is 84 mil in the Phaser® 350. Since the width of the body is nearly as long as the inlet and outlet, we also want to account for the transmission time across the body.

Rather than using a transmission line to model the body, we will instead divide the body into multiple lumped parameter segments across its width. This is analogous to what one does when applying a finite difference model, when the problem is discretized in space [7, p. 25]. If enough lumped-parameter segments are used, the solution approaches the transmission line results. The multi-segment, lumped parameter model is used instead of the transmission

line model because the body needs to be coupled with the mechanical elements of the driver (diaphragm and PZT) as well as the neighboring section(s) of body. This is difficult to do with the transmission line equations since the end boundary condition (Z_e, which is imbedded in the transmission line equation for a pipe) is now much more complicated than a single pipe boundary. The circuit model is more easily created if the body is described with lumped-parameter elements. For the model used in this study, the body and driver are divided into ten lumped-parameter segments. As a final note, the resistance of the body is still very small compared with inductance and capacitance so it will be neglected and the body modeled using L and C only.

We will refer to the improved model with transmission line representations of the inlet and outlet and multiple-lumped-parameter segments for the body as the "transmission line model". A schematic of the transmission line model of an ink jet is shown in Figure 3. For simplicity, only two driver segments are shown.
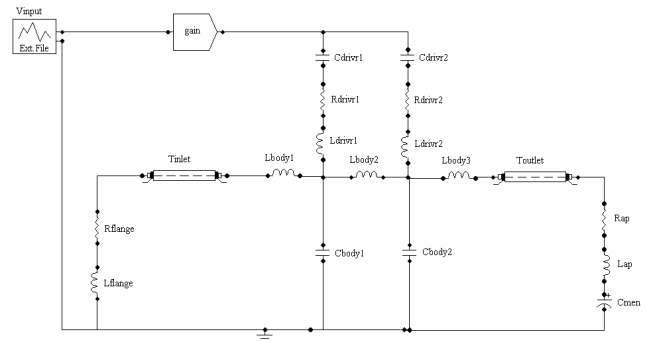

Figure 3. Schematic of transmission line ink jet model

To analyze the frequency response on the ink jet we obtain the equivalent circuit impedance for the ink jet model. The impedance is defined at the ink jet driver (at the exit of the gain amplifier in Figures 2 and 3). The equivalent impedance, Z_{jet}, can be represented as

$$Z_{jet} = Z_{drvr} + \frac{1}{A_{body} + A_{in} + A_{out}} \tag{11}$$

Z_{drvr} is the mechanical impedance of the driver. A_{body}, A_{in} and A_{out}, are the admittances (inverse impedance) of the body, total inlet and total outlet. The total inlet refers to equivalent fluid impedance of the inlet pipe and the inlet boundary conditions. Similarly, the total outlet refers to the equivalent impedance of the outlet pipe, aperture and meniscus. The equivalent fluid impedance for the lumped-parameter model is found by appropriate series and parallel combination of elements. The transmission line model uses matrix algebra rather than straight algebra to determine Z_{jet}. Once this equivalent ink jet impedance is defined, the input impedance for any frequency can be evaluated. The model improvements required only modest increases in setup and computation time.

Experimental Comparison

An impedance meter is used to measure the frequency response of an ink jet. The impedance meter measures the real and imaginary part of a system's opposition to the flow of an alternating input current at a given frequency. The real part of the inductance, Z, is the resistance (R) and the imaginary part is the reactance (X). For the data presented here, a Hewlett-Packard 4192A impedance meter was used.

To obtain the experimental data, an entire print head is heated to operating temperature and all air is removed. A probe is attached to the circuit board at the point at which the electronics feed into individual PZTs. The impedance meter performs a frequency sweep (the step size and frequency range are defined by the user), applying a one-volt peak-to-peak sine wave at each specified frequency. The impedance meter then records the real and imaginary part of the returned signal at each frequency. The data can be presented a multitude of ways, but for comparing the data to the model predictions, the conductance (G) is plotted. Conductance is the real part of the admittance (the reciprocal of impedance). An average of four individual jets for a single head is plotted for the experimental data. Averaging jets is done to eliminate any slight variation caused by temperature and individual jet geometries and also to reduce measurement noise.

Figure 4 compares the lumped-parameter and transmission line model results with impedance meter data for a Phaser® 350 print head. Different frequency ranges are plotted in Figure 4a and 4b to better illustrate the frequency response if the ink jet. Figure 4a is the low frequency response. The experimental data shows the bulk mode of oscillation or Helmholz frequency at approximately 24 kHz. Figure 4b is the higher frequency results. The driver resonance is the large peak at around 300 kHz. The other smaller peaks (at approximately 100 kHz, 210 kHz, 265 kHz and 390 kHz) are those associated with the inlet and outlet resonance modes. There is usually one resonance associated with the inlet and outlet by themselves, and the other resonant frequencies are combinations of geometric features (e.g. the body and outlet resonating together). These resonant frequencies are often referred to as parasitic frequencies because they do not contribute to the ejection of ink drops at the aperture.

There is virtually no difference between the lumped-parameter model and transmission line model in predicting the Helmholz frequency. During the main bulk mode resonance (Helmholz) the whole jet acts as one fluid unit (as a 'lump'), so the transmission line model offers no benefit in this case. The two models are equally as accurate in predicting the driver resonance - another bulk resonance mode.

The major difference between the two models is the ability to predict the parasitic resonant frequencies. The lumped-parameter model predicts one parasitic type resonance at 150 kHz; the transmission line model predicts seven. The transmission line does a good job of accurately predicting the 110 kHz and 220 kHz resonant frequencies in

the experimental data. It does a reasonable job of predicting the mode at 380 kHz (i.e. the mode exists although the frequency is not quite accurate). There are two additional frequencies at 95 kHz and 340 kHz that the transmission line model predicts but whose amplitudes are much lower than the experimental data. The frequency of the 340 kHz peak is also lower than actual. The 150 kHz peak in the transmission line prediction also appears in the lumped parameter prediction and does not seem to correspond to any actual resonance. The 450 kHz peak in the transmission line model also does not seem to correspond to an actual frequency. These two peaks appear to be artifacts of the lumped-parameter model of the body as they significantly decrease in magnitude as discrete segments are added to the body (data not shown). This leads one to suspect that this resonance is due to the some common problem with the model implementation such as one of the boundary conditions or assumptions in deriving the governing equations.
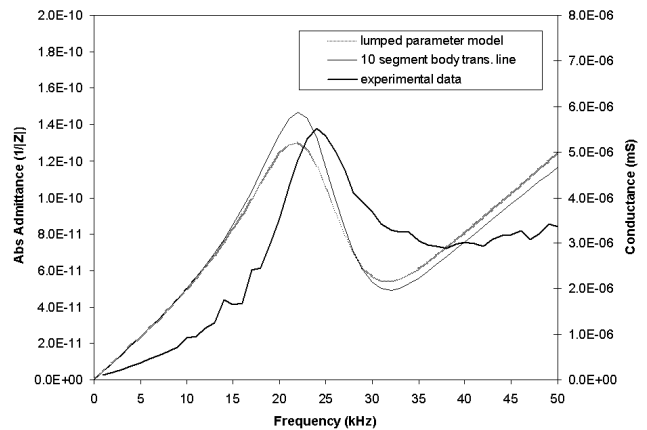
(a)
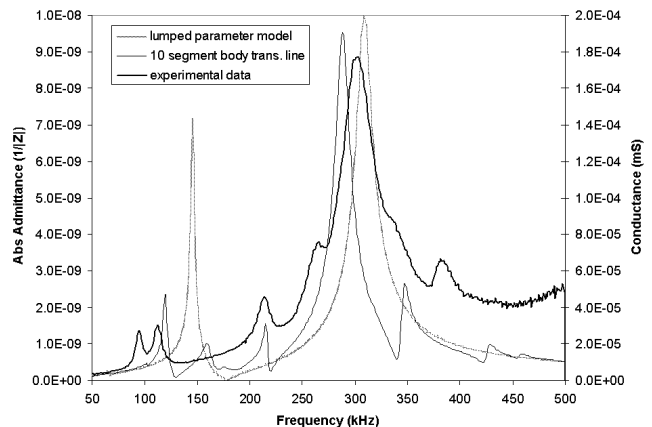
(b)

Figure 4. Frequency comparison of lumped-parameter and transmission line modlsl to experimental data for a Phaser® 350 ink jet (a) Helmholz frequency (b) Driver and parasitic frequencies

Conclusion

Comparison of the predicted frequency response of the lumped-parameter and transmission line models to experimental data for a Phaser® 350 print head shows significant improvement in predicting resonant frequencies. Both models do an adequate job of matching bulk mode resonant frequencies (the Helmholz and driver resonant modes). It is in the prediction of the parasitic frequencies that the improvements obtained with the transmission line models are most significant.

Adding the ability to simulate the time delay in pressure waves as they travel though the ink jet made these improvements possible. This was accomplished by incorporating transmission line models for the inlet and outlet geometries and by discretizing the driver to approximate transmission line effects.

The goal of the modeling effort was to improve upon the lumped-parameter model used for ink jet design. The model obtains frequency-domain solutions to quickly evaluate the dynamic response of an ink jet. The dynamic response can be used to design waveforms that apply energy at the Helmholz frequency while reducing energy at any undesirable frequencies. It can also be used to identify geometric features that cause unwanted resonant modes and to determine changes to the geometry that modify the resonance.

References

1. F.M. White, Fluid Mechanics, 2nd Ed., McGraw-Hill Book Company, New York, 1986.
2. E. B. Wylie and V. L. Streeter with L. Suo, *Fluid Transients in Systems*, Prentice-Hall, Inc., New Jersey, 1993.
3. L.E. Kinsler, A.R. Frey, A.B. Coppens, J.V. Sanders, *Fundamentals of Acoustics*, 3rd Ed., John Wiley & Sons, New York, 1982.
4. A.D. Pierce, *Acoustics: An Introduction to Its Physical Principles and Applications*, Acoustical Society of America, New York, 1991.
5. P.M. Morse and K.U. Ingard, *Theoretical Acoustics*, Princeton University Press, New Jersey, 1968.
6. J. Roy, R.L. Adams, J. Anderson, Pressure Generation in Drop-on-Demand Ink Jets, *SID International Digest of Technical Papers*, Vol. XVI, pg. 314. (1985).
7. C. Christopoulos, The *Transmission-Line Modeling Method: TLM*, IEEE Press, New Jersey, 1995.

Biography

Sharon Berger received her B.S. in Mechanical Engineering from Arizona State University in 1991 and her M.S. in Mechanical Engineering from Portland State University in 2003. She has worked for the past eleven years at the Xerox Office Products Group (formerly the Color Printing and Imaging Division of Tektronix) where she is currently a senior mechanical engineer in Ink Jet Development for Phase Change Research and Development. Her present responsibilities and interests are in the design and performance of phase change ink jet print heads. She has co-authored four papers in that area and is an inventor on four issued patents and one patent pending.